The SNARE Machinery Is Involved in Apical Plasma Membrane Trafficking in MDCK Cells

Seng Hui Low,* Steven J. Chapin,* Christian Wimmer,[§] Sidney W. Whiteheart,[‖] László G. Kömüves,[‡] Keith E. Mostov,* and Thomas Weimbs*

*Department of Anatomy, Department of Biochemistry and Biophysics, Cardiovascular Research Institute,[‡]Department of Dermatology and Veteran Administration Medical Center, University of California, San Francisco, California 94143-0452; [§]Department of Cellular Biochemistry and Biophysics, Memorial Sloan-Kettering Cancer Center, New York 10021; [‖]Department of Biochemistry, University of Kentucky College of Medicine, Lexington, Kentucky 40536

Abstract. We have investigated the controversial involvement of components of the SNARE (soluble *N*-ethyl maleimide–sensitive factor [NSF] attachment protein [SNAP] receptor) machinery in membrane traffic to the apical plasma membrane of polarized epithelial (MDCK) cells. Overexpression of syntaxin 3, but not of syntaxins 2 or 4, caused an inhibition of TGN to apical transport and apical recycling, and leads to an accumulation of small vesicles underneath the apical plasma membrane. All other tested transport steps were unaffected by syntaxin 3 overexpression. Botulinum neurotoxin E, which cleaves SNAP-23, and antibodies against α-SNAP inhibit both TGN to apical and basolateral transport in a reconstituted in vitro system. In contrast, we find no evidence for an involvement of *N*-ethyl maleimide–sensitive factor in TGN to apical transport, whereas basolateral transport is NSF-dependent. We conclude that syntaxin 3, SNAP-23, and α-SNAP are involved in apical membrane fusion. These results demonstrate that vesicle fusion with the apical plasma membrane does not use a mechanism that is entirely unrelated to other cellular membrane fusion events, but uses isoforms of components of the SNARE machinery, which suggests that they play a role in providing specificity to polarized membrane traffic.

The SNARE[1] (soluble *N*-ethyl maleimide–sensitive factor [NSF] attachment protein [SNAP] receptor) hypothesis provides a universal model of how nearly all intracellular membrane fusion events work (12, 21, 40, 41, 43). The essentials of the original version of the model are that v-SNARE proteins located on vesicles bind to t-SNARE proteins located on target membranes. In a mechanism that is not well understood, this binding leads ultimately to the fusion of the membranes of vesicle and target. Several soluble proteins, such as the ATPase NSF and α-SNAP interact with the v- and t-SNAREs and are thought to be general factors involved at some point(s) in the overall membrane traffic process. The SNARE hypothesis proposes not only that the SNARE machinery accomplishes the membrane fusion event but that it also plays a major role in the specificity of membrane fusion. To this goal, the correct pairing of individual members of the large family of v-SNAREs with corresponding members of the large family of t-SNAREs would be required before fusion can occur. Indeed, different isoforms of v- and t-SNAREs have been shown to be involved in different membrane traffic pathways (12, 21, 41, 43). This is reflected by the different subcellular localizations of distinct SNARE isoforms.

Recently, analysis of membrane traffic in polarized epithelial cells has provided evidence of another membrane fusion mechanism, which has been suggested to be wholly unrelated to the SNARE hypothesis (23). Polarized epithelial cells have two plasma membrane domains, apical and basolateral. Newly made membrane proteins can reach these surfaces by two pathways. (*a*) Proteins can be sent from the TGN directly to either the apical or basolateral surface. (*b*) Proteins can first be sent to one surface (usually the basolateral) and from there are endocytosed and transcytosed to the apical surface (31). Ikonen et al. (23) investigated the involvement of several components

Address all correspondence to Keith Mostov, University of California, San Francisco, Department of Anatomy, San Francisco, CA 94143-0452. Tel.: (415) 476-6048. Fax: (415) 476-4845. E-mail: mostov@itsa.ucsf.edu

1. *Abbreviations used in this paper*: BoNT, botulinum neurotoxins; GPI, glycosylphosphatidylinositol; NEM, *N*-ethyl maleimide; NSF, *N*-ethyl maleimide–sensitive factor; pIgR, polymeric immunoglobulin receptor; SL, Signal-less; SLO, streptolysin-O; SNAP, soluble NSF attachment protein; SNAP-25, synaptosomal-associated protein of 25 kD; SNARE, SNAP receptor; WT, wild-type.

of the SNARE machinery in direct delivery from the TGN to the apical and basolateral surface. These authors reconstituted delivery from the TGN to either surface in polarized MDCK cells that had been permeabilized with the pore-forming toxin streptolysin-O (SLO). It was shown that TGN to basolateral surface transport behaved as predicted by the SNARE hypothesis: transport was inhibited by antibodies to NSF, stimulated by recombinant α-SNAP, inhibited by neurotoxins that proteolytically cleave the v-SNARE synaptobrevin/VAMP-2, and inhibited by Rab-GDI, which sequesters and inhibits Rab proteins that probably act upstream of SNAREs. Remarkably, all of these treatments were without effect on TGN to apical transport (23). The transport vesicles involved in this step are very enriched, however, in annexin 13b, and antibodies to annexin 13b inhibit reconstituted TGN to apical transport (19). These data led to the suggestion that TGN to apical transport uses a completely novel mechanism, whose only known positive attribute is the involvement of annexin 13b (42). One conclusion from this model is that specificity in basolateral versus apical membrane transport is conferred by the complete incompatibility of the fusion machineries rather than by a combinatorial pairing of SNAREs and/or their associated proteins (52).

TGN to apical transport thus stands as the most credible exception to the universality of the SNARE hypothesis (and its variants). The proposed existence of an alternative mechanism has attracted a great deal of ongoing attention, as it has profound consequences for our understanding of membrane traffic. For instance, the genome of *Saccharomyces cerevisiae* encodes eight recognizable classical members of the syntaxin family of t-SNARE subunits (22, 49) each of which may identify a unique compartment. This may be the most meaningful way in which to define a membrane compartment. The existence of a non-SNARE fusion mechanism would, of course, allow the existence of other compartments, not necessarily defined by a t-SNARE. Furthermore, TGN to apical transport has been proposed to use glycolipid- and cholesterol-rich membrane microdomains, "rafts" (42). The involvement of a non-SNARE, annexin 13b mechanism in this transport has been, in fact, one of the principal arguments in support of the hypothesis that such TGN to apical rafts are fundamentally different from the "conventional" mode of vesicular transport (42, 48).

Two subsequent findings, however, raised doubts that vesicle fusion with the apical plasma membrane is fundamentally different from other membrane fusion events. First, Apodaca et al. (5) studied the basolateral to apical transcytosis of IgA in MDCK cells and found that the final fusion event involves NSF and can be inhibited by botulinum neurotoxin E (BoNT-E), which normally inactivates the neuronal t-SNARE SNAP-25. Although the target of the toxin was unknown at the time of that study, the interpretation of the result was that at least a subset of trafficking pathways to the apical plasma membrane (i.e., transcytosis) must involve the SNARE machinery. Second, we and others have found that certain t-SNARE isoforms are localized to the apical PM of epithelial cells (for review see reference 48). At least at the plasma membrane, the t-SNARE consists of two subunits, which are members of the syntaxin and SNAP-25 families, respectively. Three syntaxin isoforms could be identified at the plasma membrane of MDCK cells: syntaxin 2 is found at both the basolateral and apical surface, whereas syntaxins 3 and 4 are localized to the apical or basolateral membranes, respectively, with no overlap (26). This result suggested (*a*) that the apical plasma membrane does use components of the SNARE machinery and (*b*) that syntaxins 3 and 4 may serve specific pathways to either membrane. We and others could also show that SNAP-23, the only known non-neuronal isoform of SNAP-25, is localized to both plasma membrane domains in MDCK cells (27) and that it is a substrate of the BoNT-E (25, 27), which makes it likely that this t-SNARE is involved at least in the fusion of transcytotic vesicles with the apical membrane.

To solve the question of the involvement of the SNARE machinery in TGN to apical plasma membrane fusion we have investigated the involvement of specific components of this machinery by functional studies. While we indeed can find no evidence for a role of NSF, we present data confirming that this pathway uses syntaxin 3, α-SNAP, and SNAP-23. We conclude that TGN to apical transport uses several of the elements of the SNARE machinery and therefore does not represent an entirely novel type of membrane fusion.

Materials and Methods

Materials, Reagents, and Recombinant Proteins

Most materials were from previously described sources (26, 27). SLO was obtained from Dr. S. Bhakdi (University of Mainz, Mainz, Germany). The generation and characterization of the mAbs 2F10 and 3E2 against α-SNAP will be described elsewhere. The antibodies were purified from ascites fluid by ammonium sulfate precipitation, protein G affinity chromatography, concentration on dry PEG 34000 and extensive dialysis against 115 mM KOAc, 20 mM Hepes-KOH, pH 7.4, 2.5 mM $MgOAc_2$, 5 mM glutathione. Antibodies against the ectoplasmic domain of rabbit pIgR generated in guinea pig (9) and sheep (3) have been described before. Recombinant wild-type and mutant (D1E-Q) NSF—both containing a myc and His_6 tag—were prepared and purified as described (51). Recombinant α-SNAP was prepared as described in (50). cDNAs for the bacterial expression of His-tagged BoNT light chains were a gift of Drs. T. Binz and H. Niemann (Medizinische Hochschule Hannover, Hannover, Germany). The toxins were expressed in *Escherichia coli* and purified as described (7). All other chemicals and reagents were from Sigma Chemical Co. (St. Louis, MO) or Boehringer Mannheim Corp. (Indianapolis, IN).

Cell Culture and Transfection of MDCK Cells

MDCK strain II cells were grown as previously described (27). For all quantitative assays cells were plated on Transwell polycarbonate filters (12-mm diam, 0.4-μm pore size; Corning-Costar Corp., Corning, NY) at high density and maintained for 3–4 d with regular media changes. The generation of MDCK clones stably expressing WT-pIgR (29), 664A-pIgR (14), SL-pIgR (15), or glycosylphosphatidylinositol (GPI)-pIgR (30) have been described previously. In the GPI-pIgR, the entire cytoplasmic domain of pIgR has been deleted. During biosynthesis, the remaining hydrophobic COOH-terminal domain is exchanged for a GPI anchor.

MDCK clones that overexpress different syntaxin isoforms were generated exactly as described before (26). Briefly, MDCK cells, expressing the WT-pIgR or different pIgR mutants, were individually transfected with pCB7 constructs containing syntaxin 2, 3, or 4 followed by selection in hygromycin. Clones were screened for syntaxin expression by Western blot and immunofluorescence microscopy. For all clones, care was taken to check that the localization of the expressed syntaxin isoforms did not differ from the localization previously reported (26). The polarity of all clones was verified as described (26) and only those clones that passed these tests were investigated further.

Measurement of Biosynthetic Transport to the Apical or Basolateral Plasma Membrane in Intact Cells

Confluent MDCK cell monolayers on polycarbonate filters were washed twice with PBS^+ and starved in MEM^- cysteine for 15 min at 37°C. Proteins were then pulse labeled by placing the Transwell on a 25-μl drop of MEM^- cysteine containing 44 μCi of [^{35}S]cysteine (sp act: 1,000 Ci/mmol) for 10 min at 37°C. Cells were washed with MEM-BSA (MEM with Hanks' salts, 0.35 g/liter $NaHCO_3$, 20 mM Hepes-Na, pH 7.4, 6 mg/ml BSA) and the chase was continued with MEM-BSA in the apical chamber and MEM-BSA containing guinea pig anti-pIgR antibody in the basal chamber for 45 min (WT-pIgR) or 40 min (SL- and GPI-pIgR). Afterwards, the cells were immediately cooled on ice for 1 h to allow for efficient antibody binding. Media were collected and the remaining unbound antibody was removed by three 10-min washes with MEM-BSA on ice. The filters were cut out and the cells solubilized by incubation at 37°C with shaking for 15 min in Mixed Micelle Buffer (MMB) (9) containing a large excess of MMB-lysate of unlabeled pIgR-expressing MDCK cells to prevent any remaining unbound antibody from binding to radiolabeled pIgR. The cleared cell lysates were immunoprecipitated first with protein A–Sepharose to recover the basolaterally transported pIgR molecules bound to guinea pig antibody and then subsequently with sheep anti-pIgR antibody coupled to protein G–Sepharose to determine the intracellular amount of pIgR. Cleaved, soluble pIgR-ectodomain in the apical media was immunoprecipitated using sheep anti-pIgR antibody coupled to protein G–Sepharose. The radiolabeled pIgR in each fraction was determined by SDS-PAGE and phosphorimaging. The pIgR molecules transported to the apical surface would be cleaved by an apical endogenous protease of MDCK cells and released into the apical media. The biosynthetic transport of pIgR to the apical surface was calculated by dividing the proportion detected in the apical media by the total amount of radiolabeled pIgR recovered from all fractions. Basolaterally transported pIgR, on reaching the basolateral surface, is bound by the antibody present in the basal media. The percentage of transport to the basolateral surface was thus determined by dividing the amount of pIgR recovered by protein A immunoprecipitation from the cell lysate by the total radiolabeled pIgR recovered from all fractions. The amount of pIgR that had not reached any surface yet was calculated by dividing the amount that was recovered in the second immunoprecipitation of the cell lysates after the antibody-bound pIgR was removed by protein A–Sepharose by the total radiolabeled pIgR.

Transcytosis and Recycling Assays

Basolateral to apical transcytosis was carried out exactly as described previously (13). The apical recycling of IgA was determined as follows. Tight cell monolayers on 12-mm Transwells were rinsed twice with MEM-BSA. Radioiodinated IgA ($1–2 \times 10^7$ cpm/μg) in 100 μl of MEM-BSA was added to the apical chamber and incubated for 10 min 37°C for internalization. The apical surface was washed four times in a total time period of 3 min with MEM-BSA. Fresh MEM-BSA at 37°C was added to both chambers and the media were replaced at various time points over a 120-min period. At the end of the time course, the radioactivity in all the media fractions and the cells was measured.

Permeabilization of MDCK Cells and Reconstitution of Transport

This procedure was carried out as described previously (23, 36), with slight modifications. Transport from the TGN to the basolateral plasma membrane was monitored using 664A-pIgR and to the apical plasma membrane using SL- or GPI-pIgR as reporter molecules. Briefly, MDCK cells expressing either of the pIgR mutants were grown on polycarbonate filters and pulsed labeled with [^{35}S]cysteine as described above, and then incubated at 17°C for 2 h to accumulate radiolabeled proteins in the TGN (28). The cells were washed twice with ice-cold KOAc buffer (20 mM Hepes-KOH, pH 7.4, 115 mM potassium acetate, 2.5 mM magnesium acetate, 0.9 mM $CaCl_2$) and once with KTM buffer (20 mM Hepes-KOH, pH 7.4, 115 mM potassium acetate, 3.5 mM magnesium acetate, 5 mM glutathione, 2 mM EGTA, 2 mM K_2CaEGTA). SLO was bound to the basolateral surfaces by placing the Transwells on a 20-μl drop of KOAc buffer containing 0.3 μg of SLO and 2 mM DTT on ice for 10 min. Excess unbound SLO was removed by washing the filters three times with ice-cold KTM. Cell permeabilization and cytosol washout was achieved by incubation at 17°C for 45 min in KTM. Transport was reconstituted by adding to the basal permeabilized side 500 μl of KTM containing an ATP-regenerating system (1 mM ATP, 8 mM creatine phosphate, 50 μg/ml creatine kinase) in the presence or absence of HeLa cell cytosol (final concentration ~4 mg/ml protein) and KTM alone in the apical chamber. Transport of pIgR to the apical or basal surface was determined by antibody capture achieved by including guinea pig antibody against the ectoplasmic domain of pIgR in the apical or basal media, respectively, and then incubating at 37°C for 60 min. Antibody binding was completed by incubation for 60 min on ice, and pIgR in the media and cells was recovered as described above by immunoprecipitation, resolved by SDS-PAGE, and then quantified by phosphorimaging. The cytosol-, ATP-, and temperature-dependence of reconstituted transport was very similar to the values published by Simons and colleagues (23, 36).

NEM Treatment of Permeabilized Cells and Addition of NSF

After [^{35}S]cysteine labeling, SLO binding, and cell permeabilization with cytosol washout at 17°C, the cells were washed twice with ice-cold KTM without glutathione. 0.05 or 0.15 mM NEM (for basolateral or apical transport, respectively) diluted in 0.5 ml KTM without glutathione was added to both the apical and basal chambers and incubated on ice for 15 min. The cells were then incubated with KTM containing 5 mM DTT for 3 min, and with regular KTM including glutathione for 5 min on ice before resuming the protocol as above. Where appropriate, 200 μg/ml of purified, recombinant myc-tagged His_6-NSF was added to the final transport buffer.

Treatment of Permeabilized Cells with NSF Mutant, BoNTs, and Anti–α-SNAP Antibody

Pulse-labeling, TGN-accumulation, SLO-binding, and permeabilization were carried out as described above. For experiments involving treatment with recombinant mutant NSF, HeLa cytosol, the ATP-regenerating system with or without 200 μg/ml recombinant mutant NSF in KTM were added to the basal chamber and left for 15 min at 17°C before warming up to 37°C and resuming as described above.

For experiments involving treatment with BoNTs, the standard protocol was used except that 10 or 100 μg/ml of purified recombinant His_6-tagged light chains of BoNT-E or—as a control—an inactive mutant of BoNT-C1, in which the glutamate residue at position 229 in the active site was exchanged for an alanine residue (54), were added to the basal chambers during the permeabilization and transport steps. As a further control, BoNT-E was inactivated by boiling for 10 min before addition to the permeabilized cells.

For experiments involving α-SNAP antibodies, 110 μg/ml of mAbs 2F10 or 3E2 were added to the basal chambers during permeabilization and transport steps. The concentration of cytosol in the transport reaction was reduced by half as compared with all other experiments to reduce the added amount of exogenous α-SNAP present in the cytosol. As a control, a fourfold molar excess of recombinant α-SNAP was added to the antibodies 10 min before they were added to the permeabilized cells.

Electron Microscopy

The fixation and imidazole-based staining procedure of Thiery et al. (44) was used with slight modifications. MDCK cells cultured for 4 d in Transwell polycarbonate filters were rinsed with PBS^+ and immediately fixed in 2.7% glutaraldehyde, 0.8% paraformaldehyde in 0.1 M cacodylate buffer, pH 7.2 for 2 h, and then stored in buffer alone at 4°C overnight. The cells were postfixed in 2.0% OsO_4, 0.05 M imidazole in 0.1 M barbital-acetate buffer, pH 7.2, at 37°C for 60 min. After washing three times for 5 min in distilled water, the cells were stained in a double lead and copper citrate solution at 37°C for 30 min, washed three times 5 min in distilled water, and then dehydrated through a series of graded ethanol (50, 70, 80, 95, and 100%). The cells were incubated in 100% ethanol/Spurr's resin (1:1) for 30 min at room temperature and then switched to 100% resin for 60 min. Polymerization was carried out overnight at 60°C. 75–85-nm sections were cut and mounted on nickel grids. No poststaining of the cells was necessary. Images were taken on a Zeiss 10 CA Electron Microscope at 60 kV.

Results

Overexpression of Syntaxin 3 Inhibits Biosynthetic Transport to the Apical but Not Basolateral Surface of MDCK Cells

We have reported previously the differential plasma membrane localization of the syntaxin isoforms 2, 3, and 4 in MDCK cells (26). To study whether any of these t-SNAREs are involved in any of the established membrane traffic pathways, we investigated the possible influence that the overexpression of these syntaxin isoforms may have on different pathways. The specific inhibition of transport pathways by overexpression of syntaxins has been reported previously in other systems (17, 18, 32, 53).

As a reporter molecule, we chose the polymeric immunoglobulin receptor (pIgR) whose trafficking in MDCK cells is well known (31). Newly synthesized wild-type (WT) pIgR travels directly from the TGN to the basolateral plasma membrane, where it can bind its ligand polymeric IgA. The receptor is then endocytosed and transcytosed across the cell to the apical surface. Here, an endogenous protease cleaves the extracellular domain of pIgR, releasing it into the apical medium. The WT-pIgR can be used to study the biosynthetic transport of the receptor to the basolateral plasma membrane, as well as basolateral to apical transcytosis, and basolateral and apical recycling of the ligand IgA. A mutant form of the pIgR, in which the basolateral targeting signal in the cytoplasmic domain has been deleted (Signal-less or SL-pIgR) is transported from the TGN directly to the apical plasma membrane (15). In another apically targeted mutant, the pIgR-ectodomain is inserted into the membrane by a GPI anchor (Low, S.H., K. Mostov, and T. Weimbs, manuscript in preparation).

Both SL- and GPI-pIgR can be used to measure the biosynthetic transport to the apical plasma membrane domain. Since SL-pIgR has a single membrane-spanning domain while GPI-pIgR is integrated in the membrane by a GPI anchor, both proteins may reach the apical plasma membrane by different routes. It has been proposed that proteins, like GPI-anchored proteins, that interact with detergent-insoluble glycosphingolipid and cholesterol-enriched rafts, would be segregated from proteins that do not partition into these rafts. We have indeed found that GPI-pIgR is partially insoluble in Triton X-100–containing buffers whereas SL-pIgR is entirely soluble (Low, S.H., K.E. Mostov, and T. Weimbs, manuscript in preparation).

The assay system we used to measure the biosynthetic transport of pIgR to the basolateral or apical plasma membrane is a pulse-chase protocol in which the basolaterally delivered receptor is detected by surface immunoprecipitation and the apically delivered receptor by release of the ectodomain into the apical medium after cleavage by the endogenous protease (see Materials and Methods).

The syntaxin isoforms 2, 3, and 4 were overexpressed by stable transfection in MDCK cells that also express either the WT-, SL-, or GPI-pIgR. The same expression vector with a cytomegalovirus (CMV)-promoter was used for all syntaxin isoforms and several individual clones were isolated that expressed similar amounts of the same syntaxin isoform in each of the parental cell lines. The extent of syntaxin overexpression over WT levels is ~10-fold (26). As shown in Fig. 1 *A*, transport of pIgR to the basolateral surface was not affected by overexpression of any of the syntaxin isoforms. In contrast, the apical transport of SL- as well as GPI-pIgR was consistently inhibited by the overexpression of syntaxin 3 but not syntaxins 2 or 4 (Fig. 1, *B* and *C*). The overexpression of syntaxin 3 did not cause mistargeting of SL- or GPI-pIgR to the basolateral

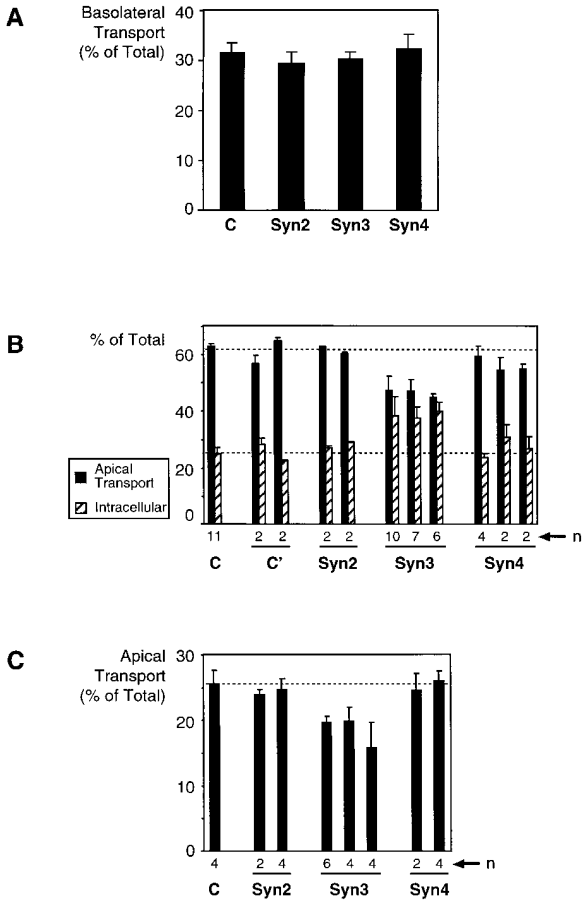

Figure 1. Effect of syntaxin overexpression on TGN to surface transport of WT-, SL-, or GPI-pIgR in MDCK Cells. (*A*) MDCK cells expressing WT-pIgR were untransfected (*C*) or stably transfected with syntaxin 2 (*Syn2*), 3 (*Syn3*), or 4 (*Syn4*). As described in Materials and Methods, newly synthesized pIgR transported to the basal surface was measured in a pulse-chase protocol and expressed as a percentage of the total labeled pIgR. The values were determined using two different clones in triplicate filters each and the means and standard deviation are plotted. (*B*) MDCK cells expressing SL-pIgR were transfected with either syntaxin 2, 3, or 4. Untransfected parental cells (*C*) or cells transfected with the syntaxin 4 plasmid but not expressing the protein (*C′*) served as controls. Transport of newly synthesized SL-pIgR was determined in a pulse-chase experiment and the amount transported to the apical surface (*black bars*) or remaining in the cell at the end of the chase (*hatched bars*) is expressed as a percentage of the total labeled SL-pIgR. Except for the control parental cell line, multiple clones of each cell line were examined and the values shown are the means and standard deviation of several filters (*n*). Dotted lines indicate the average values of the control experiments. (*C*) MDCK cells expressing GPI-pIgR were untransfected (*C*) or transfected with syntaxin 2, 3, or 4. Delivery to the surface was measured as described above. The inhibition of apical transport of SL- and GPI-pIgR by syntaxin 3 overexpression is statistically significant (Student's *t*-test, $P < 10^{-10}$).

domain but rather an intracellular accumulation that would be consistent with a kinetic perturbation of vesicle fusion. That a similar inhibition in apical transport after syntaxin 3 overexpression was observed with two different reporter molecules in several independent clones argues against an artifact of clonal variation. The finding that the apical but not the basolateral pathway was inhibited by syntaxin 3 overexpression indicates that the inhibition takes place at a post-TGN step because the transport pathways of membrane proteins are believed to be identical until they leave the TGN (20).

Overexpression of Syntaxin 3 Inhibits Apical Recycling but Not Basolateral to Apical Transcytosis of Endocytosed IgA

In addition to TGN to apical delivery, the two other known pathways to the apical surface are transcytosis from the basolateral surface, and recycling from the apical surface back to the apical surface. We used the same clones of MDCK cells, expressing WT-pIgR and the syntaxin isoforms 2, 3, and 4 as above, to measure these pathways quantitatively. Fig. 2 *A* shows that basolateral to apical transcytosis of IgA by pIgR is not affected by overexpression of syntaxins 2, 3, or 4. Recycling of IgA back to the basolateral surface was also not affected (not shown).

We also used the WT-pIgR to assay recycling of apically internalized material back to the apical surface. Although the pIgR is rapidly cleaved at the apical surface, there is always a pool of pIgR that has not yet been cleaved. We have previously shown that IgA bound to this apical pIgR is internalized and largely recycled to the apical surface (10). Fig. 2 *B* shows that overexpression of syntaxin 3, but not syntaxins 2 or 4, specifically slows apical recycling of this IgA. The rates of IgA uptake from the apical or basolateral surfaces were identical in all clones (data not shown).

Taken together, Figs. 1 and 2 show that overexpression of syntaxin 3 specifically reduces TGN to apical transport and apical recycling. This is not due to blockage of all polarized traffic (e.g., by titration of a common transport factor) as TGN to basolateral delivery and transcytosis to the apical surface are not affected. The apical recycling assay clearly shows that the effect is largely kinetic.

Despite the isolation of individual clones we never obtained completely uniform expression of the transfected syntaxins in MDCK cells, even after repeated subcloning. Based on immunofluorescence analysis, only ~50–75% of the cells in each clone expressed the transfected syntaxins at the time of our experiments, though it is possible that some of the remaining cells expressed lesser amounts of transfected syntaxin 3 that were not clearly visible above background. It is therefore, likely that the true inhibitory effect on TGN to apical delivery and apical recycling in individual cells of high syntaxin 3 expression was much greater than could be observed biochemically in the entire population. The same clones of MDCK cells expressing WT-pIgR and the syntaxin isoforms were used for the TGN to basal surface, transcytosis, and recycling assays. Since an inhibitory effect of syntaxin 3 overexpression was observed in apical recycling, this very same level of syntaxin 3 overexpression had no effect on the other two pathways.

Overexpression of Syntaxin 3 Causes Accumulation of Vesicles Near the Apical Plasma Membrane

The results described above strongly suggest that syntaxin 3, which is localized at the apical plasma membrane (26), plays a role in the two transport pathways that are affected by its over-expression. To investigate whether the observed inhibition of apical transport pathways caused morphological changes, we examined the cells, grown under the same conditions as for the transport assays, by thin-section electron microscopy. The appearance of the cells was identical and the relative volumes of cytoplasm, nuclei, mitochondria and Golgi apparatus did not differ between syntaxin 3 overexpressing and control cells (Table I). However, an increase in the number of small vesicles with a typical diameter of 100 nm (range: 50–200 nm) occurring within less than half a vesicle diameter of the apical plasma membrane was observed in cells overexpressing syntaxin 3. Results of a typical experiment are shown in Table I, in which approximately twice as many of such vesicles were observed per unit length in the syntaxin 3–overexpressing cells. This experiment was repeated several times using a variety of fixation protocols. In all cases, we obtained the same result of approximately twice as many

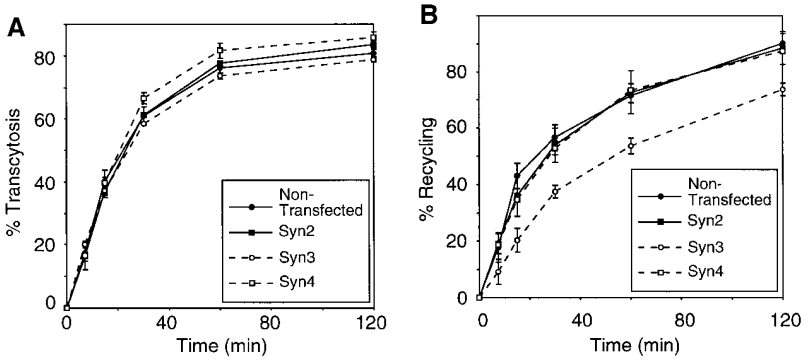

Figure 2. Transcytosis and apical recycling of IgA in syntaxin-overexpressing MDCK cells. Transcytosis and recycling pathways of IgA were analyzed in MDCK cells stably expressing WT-pIgR and syntaxins 2, 3, or 4. (*A*) For transcytosis, radioiodinated IgA was internalized from the basal surface of the cell for 10 min, washed, and then chased at 37°C. At indicated time intervals, the apical and basal media were collected, replaced with fresh media, and then incubated further at 37°C. Finally, the radioactivity of the collected media, and that remaining in the cells was determined. The values (mean and SD) of apically released radioiodinated IgA, expressed as percent of the total radioactivity, of two independent clones each in triplicate filters, were plotted. (*B*) To measure apical recycling, radioiodinated IgA was added to the apical surface of the cell and allowed to endocytose for 10 min at 37°C. Excess IgA was washed away and the cells were chased at 37°C. At indicated time intervals media were collected and the radioactivity was determined. The plot represents the percentage of IgA recycled to the apical surface (mean and SD of two independent clones each in triplicate filters).

vesicles per unit surface length in syntaxin 3 cells. A representative field of such vesicles is shown in Fig. 3 *A*, with a corresponding field from a control cell in Fig. 3 *B*. These vesicles are always close to the apical surface and occasionally even touch it but are not continuous with it. The shape of these electron-lucent vesicles is mostly spherical; tubules were almost never observed. This result is consistent with the hypothesis that these vesicles may be intermediates in the transport pathways that are inhibited by syntaxin 3 overexpression and that syntaxin 3 overexpression causes a block in vesicle fusion, not vesicle production or transport to the region of the apical surface.

NSF Involvement Can Be Demonstrated in TGN to Basolateral but Not Apical Transport

Ikonen et al. (23) reported previously that inhibitory antibodies to NSF did not inhibit the transport of the influenza virus hemagglutinin from the TGN to the apical plasma membrane in a permeabilized MDCK cell system. To test whether this NSF independence would be observed also if the pIgR variants were used as reporters, we used a very similar in vitro–reconstituted transport system. To monitor TGN to apical transport we used the SL- and GPI-pIgR and for the basolateral transport we used 664A-pIgR in which a phosphorylation site (serine 664) in the basolateral targeting signal of the receptor is substituted with an alanine residue. This mutant receptor is transported to the basolateral surface as efficiently as the wild-type receptor but is deficient in subsequent transcytosis to the apical surface (15), which prevents any overlapping signal from transcytosis.

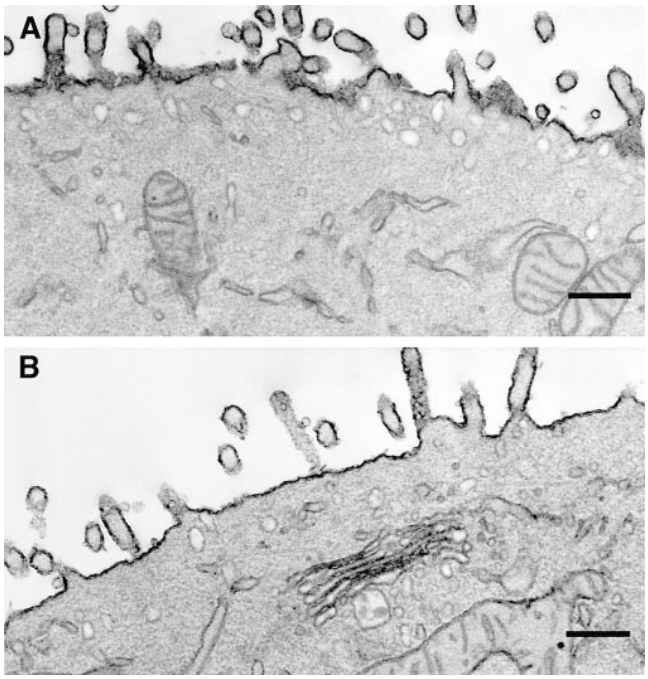

Figure 3. Small vesicles accumulate close to the apical plasma membrane in MDCK cells over-expressing syntaxin 3. MDCK cells stably transfected for syntaxin 3 (*A*) or the parental cells (*B*) were grown in parallel as tight monolayers on polycarbonate filters. Cells were processed for transmission electron microscopy. Parts of the apical plasma membrane with microvilli are shown. Small vesicles typically 100 nm in diameter can be seen close to the plasma membrane. The numbers of these vesicles are increased significantly in cells overexpressing syntaxin 3 (see Table I). Bar, 500 nm.

Table I. Analysis of the Ultrastructure of MDCK Cells Overexpressing Syntaxin 3

	Cytoplasm*	Nuclei*	Mitochondria‡	Golgi apparatus‡	Apical Vesicles/μm
Control-MDCK	64.3 (0.5)	35.7 (0.5)	7.8 (0.1)	2.8 (0.1)	0.15 (0.05)
Syn3-MDCK	65.2 (0.9)	34.8 (0.9)	7.9 (0.2)	2.9 (0.2)	0.30 (0.04)

MDCK cells overexpressing syntaxin 3 or control cells were analyzed by transmission electron microscopy. For the analysis of possible gross morphological changes, 25 microscopic fields at low magnification (5,000×) were chosen and the relative volumes of the cytoplasm versus nucleus and of the mitochondria and Golgi-apparatus were determined by point counting stereology as described by Weibel et al. (47). For the quantitation of apical vesicles, 54 (control: 28) microscopic fields at high magnification (16,000×) along the apical plasma membranes of the cell layer were collected randomly. Vesicles of a typical diameter of 100 nm (range 50–200 nm) that were 30 nm or closer to the apical plasma membrane were counted (syn3: 88; control: 22). The base of the apical plasma membrane (excluding the microvilli) was measured (syn3: 291.5 μm; control: 149.1 μm). The final values are the means (standard error) of vesicles per micrometer of base of the apical plasma membrane. The increase in the number of apical vesicles in syntaxin 3 overexpressing cells was statistically significant ($P < 0.01$ by Student's *t* test).

*Percent of total cell volume (SEM).

‡Percent of volume of cytoplasm (SEM).

§Vesicles 30 nm or closer to the apical plasma membrane (SEM).

MDCK cells expressing either of the pIgR forms were pulse-labeled and membrane proteins were transported to and accumulated in the TGN by a low temperature chase. The basolateral plasma membrane was then permeabilized using SLO and the endogenous cytosol was washed out. After the addition of exogenous HeLa cell cytosol and ATP as an energy source, transport to the plasma membrane was restored by chasing at 37°C, and radiolabeled pIgR molecules arriving at the surface were detected by surface immunoprecipitation as before. Under these conditions TGN to surface transport is energy-, cytosol-, and temperature-dependent, very similar as described previously (23, 36). Note that the cytosol-independent signal, which is due to incomplete permeabilization and cytosol washout, was not subtracted in Figs. 4–6. Therefore, an inhibition to minus-cytosol levels is identical to a 100% inhibition in Ikonen et al. (23).

To examine the involvement of NSF, we took advantage of a mutant form of NSF that binds ATP but cannot hydrolyze the nucleotide. This mutant NSF remains in its activated state and forms 20S complexes but does not disassemble them, thereby inhibiting NSF-dependent fusion events (51). As shown in Fig. 4 *A*, when added together with the exogenous cytosol to the assay, this mutant NSF inhibited TGN to basolateral surface transport of 664A-pIgR strongly (>85% of the cytosol-dependent signal), whereas it had no effect on the apical transport of SL- or GPI-pIgR.

We also performed the reverse experiment. After SLO permeabilization, the endogenous NSF was inactivated by treatment with *N*-ethyl maleimide (NEM) and recombinant, wild-type NSF was supplied afterwards together with the HeLa cytosol to overcome the inhibition. As shown in Fig. 4 *B*, TGN to basolateral transport of 664A-pIgR was completely inhibited by treatment with 0.05 mM NEM,

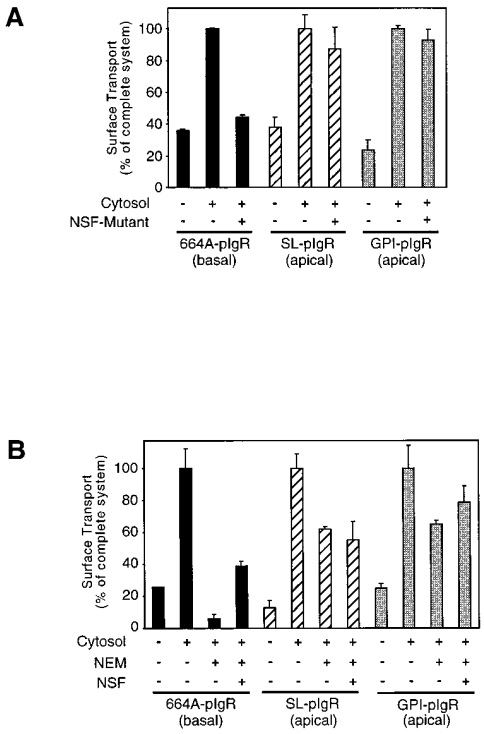

Figure 4. NSF is involved in transport from the TGN to the basolateral but not to the apical plasma membrane. (*A*) TGN to basolateral or apical plasma membrane transport was reconstituted in SLO-permeabilized MDCK cells expressing either 664A-, SL-, or GPI-pIgR as reporter molecules. The cytosol dependence of the transport reaction is shown. Addition of a recombinant, ATPase-deficient mutant of NSF (inhibits NSF-dependent fusion reactions by competition with endogenous wild-type NSF) together with the cytosol inhibits transport of 664A-pIgR to the basolateral surface strongly, while it has no effect on the apical transport of SL- or GPI-pIgR. (*B*) The reverse experiment was done by first inhibiting the endogenous NSF in SLO-permeabilized MDCK cells by treatment with 0.05 or 0.15 mM NEM (for basolateral or apical transport, respectively). NEM treatment inhibited basolateral transport of 664A-pIgR strongly whereas a threefold higher NEM concentration inhibited apical transport of SL- or GPI-pIgR only partially. Addition of recombinant wild-type NSF could partially restore basolateral transport of 664A-pIgR after NEM treatment but not apical transport of SL- or GPI-pIgR. The complete reactions (+ *Cytosol*) were set to 100%, and the values represent the mean and range of representative experiments done with duplicate filters.

and this inhibition could be partially rescued by the subsequent addition of NSF. In contrast, TGN to apical transport was much more resistant to treatment with NEM. A threefold higher concentration of NEM inhibited TGN to apical transport of SL- and GPI-pIgR only partially and this inhibition could not be overcome by the addition of NSF. These results confirm the previous observation that NSF involvement can be demonstrated only in TGN to basolateral but not TGN to apical transport (23).

α-SNAP Is Involved in TGN to Basolateral and Apical Transport

To examine the possible involvement of the second soluble constituent of the SNARE machinery, α-SNAP, in polarized transport, we took advantage of two newly developed mAbs specifically immunoprecipitating α-SNAP from HeLa and MDCK cells (Wimmer, C., and J. Rothman, manuscript in preparation). Fig. 5 shows that both antibodies inhibit TGN to basolateral transport of 664A-pIgR and TGN to apical transport of SL-pIgR in our permeabilized cell assay. This inhibition can be prevented by the addition of an excess of recombinant α-SNAP to the antibodies before they are added to the permeabilized cells. We conclude that α-SNAP or a molecule that is immunologically and functionally related is involved not only in TGN to basolateral but also apical transport.

SNAP-23 Is Involved in TGN to Basolateral and Apical Transport

Finally, we investigated whether SNAP-23, the t-SNARE that is expressed at the basolateral and apical plasma membrane domains of MDCK cells (27), would function in TGN to surface transport. Canine SNAP-23 can be cleaved by BoNT-E in analogy to the neuronal isoform SNAP-25 (27). We added recombinant BoNT-E light chain to our reconstituted transport assay, which resulted in cleavage of nearly all of the endogenous SNAP-23 by the end of the assay (data not shown). Fig. 6 shows that this treatment caused an inhibition of TGN to basolateral transport of 664A-pIgR, as well as TGN to apical transport of SL-pIgR and GPI-pIgR. The apical transport, especially of SL-pIgR, was less susceptible to treatment with BoNT-E, though the inhibition was still statistically significant and comparable to the previously reported effect of BoNT-E on transcytosis to the apical surface (5). The ad-

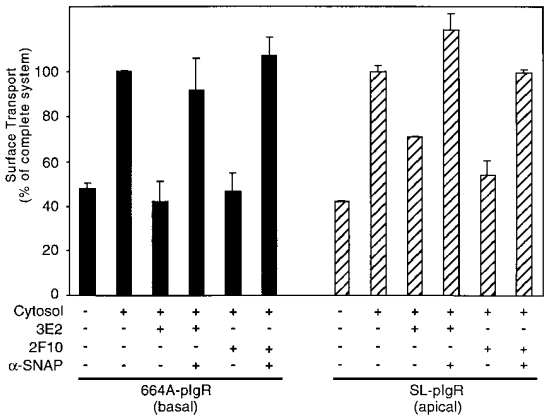

Figure 5. Antibodies against α-SNAP inhibit transport from the TGN to the basolateral and apical plasma membrane. TGN to basolateral or apical plasma membrane transport was reconstituted in SLO-permeabilized MDCK cells expressing either 664A- or SL-pIgR as reporter molecules. Addition of 110 μg/ml of the mAbs 3E2 or 2F10 against α-SNAP inhibited both the basolateral and apical transport pathways. This inhibition was completely abolished when a fourfold molar excess of recombinant α-SNAP was added to the antibodies 10 min before addition to the permeabilized cells. Note that in these experiments, the concentration of HeLa cytosol, which contains α-SNAP, was reduced by half, which also reduces the cytosol stimulation of the transport reaction. The complete reactions (+ *Cytosol*) were set to 100% and the values represent the mean and range of representative experiments done with duplicate filters.

dition of heat-inactivated BoNT-E light chain or an inactive mutant of BoNT-C1 as controls had no effect. This result suggests that SNAP-23 (or a closely related substrate for E toxin present in MDCK cells) is involved in TGN to apical transport.

Discussion

Effects of Syntaxin Overexpression

We found that the overexpression of the apical plasma membrane SNARE syntaxin 3 caused a specific inhibition of two pathways to the apical surface: biosynthetic transport from the TGN and the endocytic recycling pathway from apical endosomes. This raises the question why the overexpression of a wild-type t-SNARE would cause an inhibition of a membrane traffic pathway. Similar effects have been observed previously. The overexpression of the Golgi SNARE syntaxin 5 specifically inhibited ER to Golgi transport (17, 18). Similarly, overexpression of syntaxin 1A by transient transfection has been shown to inhibit the glucose-stimulated—but not the unstimulated—insulin secretion in pancreatic island cells, whereas the overexpression of syntaxin 1B (which is not normally expressed in β cells) had no effect (32). Finally, the overexpression of syntaxin in *Drosophila* caused a specific inhibition of neurotransmitter release by a block in synaptic vesicle fusion (53). In these cases no effect on other transport pathways was observed, which suggests that the overexpression of a particular SNARE affects only or most severely the transport step that originally involves this SNARE. The reason for such an inhibition is not completely clear, and most likely will not be well understood until the molecular mechanism by which SNAREs and other molecules catalyze membrane fusion is more thoroughly understood. However, it is clear that membrane fusion requires the sequential assembly and disassembly of several protein complexes involving SNAREs. One possible explanation for the observed inhibition is that the stoichiometry of SNARE components is disturbed, leading to a sequestration of an essential component. It is also possible that the majority of syntaxin 3 is unable to find a binding partner (possibly SNAP-23) to form a functional t-SNARE and that the non-functional t-SNAREs cannot mediate vesicle fusion although they still may allow vesicle docking. Whatever the exact molecular explanation may be, our data indicating that syntaxin 3 overexpression causes an intracellular accumulation and slows release of apically transported material are compatible with a kinetic inhibition of the fusion of transport vesicles with the apical plasma membrane. Clearly, syntaxin 3 overexpression does not block membrane traffic non-specifically as TGN to basolateral delivery and transcytosis to the apical surface are not affected.

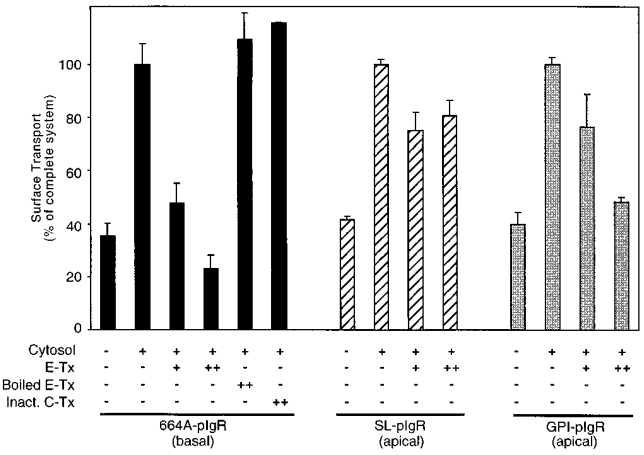

Figure 6. BoNT-E, which cleaves SNAP-23, inhibits transport from the TGN to the basolateral and apical plasma membranes. TGN to basolateral or apical plasma membrane transport was reconstituted in SLO-permeabilized MDCK cells expressing either 664A-, SL-, or GPI-pIgR as reporter molecules. The reactions were carried out in the absence or presence of 10 (1) or 100 (11) μg/ml of purified recombinant light chains of BoNT-E or an inactive mutant of BoNT-C1. Addition of BoNT-E caused inhibition of both basolateral and apical transport reactions. Inactivation of BoNT-E before addition by boiling prevented this inhibition. Similarly, addition of the inactive mutant of BoNT-C1, which served as a negative control for possible bacterial contaminants from the purification of the toxins, had no inhibitory effect. The complete reactions (+ *Cytosol*) were set to 100% and the values represent the mean and range of representative experiments done with duplicate filters. Note that in three independent experiments even the weaker inhibition of apical transport of SL-pIgR was still statistically significant by Student's *t*-test ($P < 0.002$).

The overexpression of syntaxins 2 and 4 did not affect any of the transport steps to the apical or basolateral plasma membranes that were measured. The reason may be that these syntaxin isoforms may not be involved in these pathways or, perhaps more likely, that the extent of overexpression that could be achieved with our expression system was not sufficient to disturb these pathways.

Surprisingly, apical recycling but not basolateral-to-apical transcytosis of internalized IgA was inhibited by syntaxin 3 overexpression. It had been previously reported that IgA molecules internalized from the basolateral or apical surface partially colocalize in an apical recycling compartment before they are transported to the apical plasma membrane (4). Our finding that only apical recycling, and not transcytosis, is slowed by syntaxin 3 overexpression suggests that the delivery of these molecules from the apical recycling compartment to the cell surface may be by different mechanisms. This is consistent with the previous observation that these two processes have differential sensitivities to BFA and cholera toxin (6).

It is tempting to speculate that the small vesicles of ~100-nm diam, which accumulated close to the apical plasma membrane in MDCK cells overexpressing syntaxin 3 are intermediates in the TGN to apical and/or apical recycling pathways. To our knowledge, the vesicles involved in fusion with the plasma membrane in these pathways have not previously been identified in intact mammalian cells. However, disruption of the yeast plasma membrane syntaxins Sso1p and Sso2p results in a very similar accumulation of transport vesicles of 100-nm diam (1). Putative apical transport vesicles of an average diameter of 78 nm have been purified after in vitro generation in permeabilized MDCK cells (46). It has been proposed recently that TGN-derived axonal transport vesicles are long tubules rather than small spheres (33). The small size of the vesicles we have observed makes it difficult to convincingly la-

bel them with markers of the endocytic or exocytic pathways. Therefore, we are presently unable to distinguish whether the vesicles are in the TGN to apical pathway, apical recycling pathway, or another pathway(s).

Involvement of Other Components of the SNARE Machinery

For our investigation of the involvement of NSF, α-SNAP, and SNAP-23 in biosynthetic plasma membrane transport, we have used a reconstituted transport assay in SLO-permeabilized MDCK cells that is very similar to the system previously used by Simons and colleagues (23, 36). Using two complementary approaches we found no evidence for an involvement of NSF in apical transport whereas basolateral transport was clearly NSF dependent. This result is in agreement with the antibody inhibition experiments by Ikonen et al. (23) and strongly suggests that the reported NSF independence of TGN to apical plasma membrane transport is not a peculiarity of the trafficking of the influenza virus hemagglutinin in virally infected MDCK cells but extends to at least two additional marker proteins (a GPI-anchored protein, GPI-pIgR; and a membrane-spanning protein, SL-pIgR), and may therefore be valid for TGN to apical transport in general. It seems unlikely that the observed NSF independence of the apical pathway is an artifact because (*a*) apical transport was much less sensitive than basolateral transport to treatment with NEM (Fig. 4) that, as a very small molecule, should be able to reach and inactivate NSF molecules throughout the cell with equal efficiency; (*b*) the NSF dependence of basolateral-to-apical transcytosis could be demonstrated previously by experiments very similar to ours (5). However, we can not rigorously exclude the possibility that, for some technical reason, NSF can be inhibited only at certain locations within the cell.

Our inhibition experiments using α-SNAP antibodies and the BoNT-E demonstrate that α-SNAP and SNAP-23 are involved in both TGN to basolateral as well as apical transport. Interestingly, apical transport (especially of SL-pIgR) seemed to be less sensitive to BoNT-E treatment than basolateral transport, although still statistically significant and comparable to the previously observed inhibition of transcytosis (5). It is possible that the apical plasma membrane is less accessible to the toxin or that a fraction of the transport had already passed the toxin-sensitive step. The involvement of SNAP-23 in transport to both plasma membrane domains is compatible with its localization at both domains (27). Since SNAP-23 can bind to syntaxins 1–4 with equal efficiency in vitro (39), this result suggests that it may be a general binding partner of the various syntaxin isoforms that in turn may confer specificity to vesicle fusion as suggested by their differential localization (26).

The only discrepancy between the data of Ikonen et al. (23) and ours is the involvement of α-SNAP in TGN to apical transport. This may be explained by technical differences. Ikonen et al. added recombinant α-SNAP to their transport system and noticed a stimulation of TGN to basolateral but not to apical transport. It is possible, though, that the requirement for α-SNAP of the apical pathway is lower and that the amount of α-SNAP present in the exogenous cytosol added to their system was already sufficient for maximal transport. On the other hand, our observed inhibition of apical transport by the addition of either of two different monoclonal antibodies to α-SNAP is very direct evidence for the involvement of α-SNAP.

In their original report, Ikonen et al. (23) found that the addition of tetanus toxin and BoNT-F, both of which cleave an MDCK homologue of the v-SNARE synaptobrevin/VAMP-2, to SLO-permeabilized MDCK cells inhibits basolateral but not apical transport from the TGN (23). Given the recently published localization of the plasma membrane syntaxins in MDCK cells (26) and the finding that synaptobrevin/VAMP-2 binds in vitro to the basolateral syntaxin 4 but not to the apical syntaxins 2 and 3 (11, 35), it seems only natural that apical membrane fusion should not involve synaptobrevin/VAMP-2 and therefore is toxin insensitive. We suggest that the apical syntaxins bind to different, so far uncharacterized and probably toxin-insensitive, homologues of synaptobrevin/VAMP. Several new v-SNARE homologues can be found in EST databases (8, 16) that lack the cleavage sequences for tetanus toxin, BoNT-F, and other BoNTs.

A Model of the Role of the SNARE Machinery in Polarized Membrane Traffic

Our findings lead us to propose that all membrane traffic pathways to the plasma membrane in MDCK—and probably all other—cells use the SNARE machinery for membrane fusion. Combining the results presented by Ikonen et al. (23), Apodaca et al. (5), and this paper, the following model emerges (Fig. 7). TGN to basolateral transport involves synaptobrevin/VAMP-2, α-SNAP, NSF, and

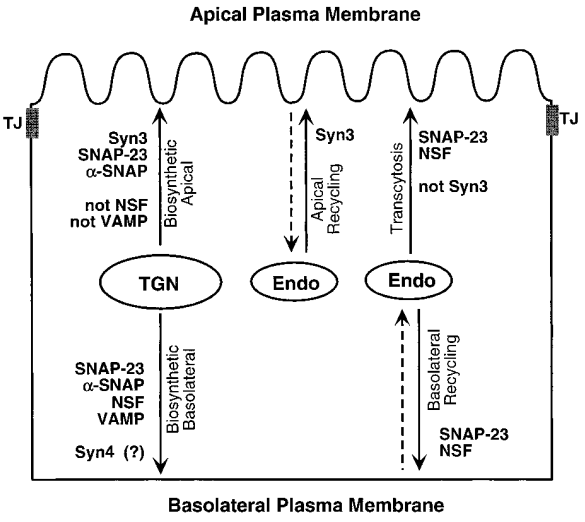

Figure 7. Model and summary of the involvement of components of the SNARE fusion machinery in polarized membrane traffic in MDCK cells. The results of this and other studies (5, 23, 27) are summarized schematically. The following pathways to the plasma membrane are depicted: biosynthetic transport (*left*), apical recycling (*middle*), basolateral to apical transcytosis (*right*) and basolateral recycling (*right*). Evidence for the involvement of one or more SNARE components has been found for each transport step. For details refer to the Discussion. *TJ*, tight junction; *Endo*, endosome.

SNAP-23. Since synaptobrevin/VAMP-2 binds in vitro only to syntaxin 4 (11, 35), and since syntaxin 4 is specifically localized to the basolateral plasma membrane domain (26), this pathway probably also involves syntaxin 4. TGN to apical transport also uses α-SNAP and SNAP-23, but involves syntaxin 3 instead of syntaxin 4. Neither NSF nor synaptobrevin/VAMP-2 are involved in this pathway. The only known feature of the apical recycling pathway is the involvement of syntaxin 3. In contrast, basolateral to apical transcytosis does not involve syntaxin 3, but does use SNAP-23 and NSF. Hence, the SNARE complex that involves syntaxin 3 excludes NSF, although α-SNAP appears to be involved. This is in agreement with the previous finding that only syntaxin 4 but not syntaxins 2 or 3 coimmunoprecipitated with NSF from membrane extracts from adipose cells, although all three syntaxin isoforms were present in the starting material (45). We suggest that in the case of apical plasma membrane fusion a homologue of NSF performs a similar function. NSF belongs to a large protein family of ATPases and homologues are involved in certain membrane fusion reactions (2, 24, 37). Interestingly, it has been established in two recent publications that syntaxins (syntaxin 5 and Ufe1p) can function not only in complexes involving NSF but also involving NSF homologues (34, 38). In these two cases (homotypic Golgi and ER fusion, respectively) no involvement of v-SNAREs or α-SNAP was found. Apparently, the SNARE fusion machinery has still surprises to offer and the existence of an NSF-independent apical SNARE machinery does not seem unlikely. So far, the only known target of α-SNAP is NSF and it will be a challenge for the future to identify such a NSF homologue that may act, together with α-SNAP, in apical membrane fusion.

Based on our data we can neither confirm nor exclude the possibility that annexin 13b plays a role in apical membrane fusion (19). It is possible that a certain fraction of apical membrane traffic can use a non-SNARE machinery. More likely, annexin 13b is required for apical transport in addition to the SNARE machinery, perhaps at a stage before SNARE assembly.

In conclusion, we demonstrated that TGN to apical plasma membrane transport is not an exception to the universal role of the SNARE machinery in intracellular membrane fusion events. Different components of the SNARE machinery are used in different membrane traffic pathways, which is likely to provide a means for ensuring the specificity of membrane fusion.

We thank J. Rothman (Memorial Sloan-Kettering Cancer Center, New York) for helpful discussions; J.-P. Vaerman (Catholic University of Louvain, Brussels, Belgium) for IgA; T. Binz and H. Niemann (Medizinische Hochschule Hannover, Germany) for cDNAs encoding BoNTs; M. Zhang for excellent technical assistance; and S. Huling (Liver Center Core Facility, UCSF-VAMC) for excellent technical help with EM.

S.H. Low and T. Weimbs were supported by the Irvington Institute for Immunology; T. Weimbs by a Feodor-Lynen-Fellowship of the Alexander von Humboldt-Foundation; S. Chapin by an American Cancer Society postdoctoral fellowship (PF3666) and an National Institutes of Health (NIH) institutional NRSA (T32HL07731); C. Wimmer by a postdoctoral fellowship from the Deutsche Forschungsgemeinschaft. This work was supported by NIH grants R01 AI25144, AI39161 to K.M. and NIH grants HL56652 to S.W.

Received for publication 2 April 1998 and in revised form 26 May 1998.

References

1. Aalto, M.K., H. Ronne, and S. Keranen. 1993. Yeast syntaxins Sso1p and Sso2p belong to a family of related membrane proteins that function in vesicular transport. *EMBO (Eur. Mol. Biol. Organ.) J.* 12:4095–4104.
2. Acharya, U., R. Jacobs, J.M. Peters, N. Watson, M.G. Farquhar, and V. Malhotra. 1995. The formation of Golgi stacks from vesiculated Golgi membranes requires two distinct fusion events. *Cell.* 82:895–904.
3. Apodaca, G., B. Aroeti, K. Tang, and K.E. Mostov. 1993. Brefeldin-A inhibits the delivery of the polymeric immunoglobulin receptor to the basolateral surface of MDCK cells. *J. Biol. Chem.* 268:20380–20385.
4. Apodaca, G., K.A. Katz, and K.E. Mostov. 1994. Receptor-mediated transcytosis of IgA in MDCK cells via apical endosome. *J. Cell Biol.* 125:67–86.
5. Apodaca, G., M.H. Cardone, S.W. Whiteheart, B.R. DasGupta, and K.E. Mostov. 1996. Reconstitution of transcytosis in SLO-permeabilized MDCK cells: existence of an NSF-dependent fusion mechanism with the apical surface of MDCK cells. *EMBO (Eur. Mol. Biol. Organ.) J.* 15: 1471–1481.
6. Barroso, M., and E.S. Sztul. 1994. Basolateral to apical transcytosis in polarized cells is indirect and involves BFA and trimeric G protein sensitive passage through the apical endosome. *J. Cell Biol.* 124:83–100.
7. Binz, T., J. Blasi, S. Yamasaki, A. Baumeister, E. Link, T.C. Südhof, R. Jahn, and H. Niemann. 1994. Proteolysis of SNAP-25 by types E and A botulinal neurotoxins. *J. Biol. Chem.* 269:1617–1620.
8. Bock, J.B., and R.H. Scheller. 1997. Protein transport. A fusion of new ideas [news; comment]. *Nature.* 387:133–135.
9. Breitfeld, P., J.E. Casanova, J.M. Harris, N.E. Simister, and K.E. Mostov. 1989. Expression and analysis of the polymeric immunoglobulin receptor. *Methods Cell Biol.* 32:329–337.
10. Breitfeld, P.P., J.M. Harris, and K.E. Mostov. 1989. Postendocytotic sorting of the ligand for the polymeric immunoglobulin receptor in Madin-Darby canine kidney cells. *J. Cell Biol.* 109:475-486.
11. Calakos, N., M.K. Bennett, K.E. Peterson, and R.H. Scheller. 1994. Protein–protein interactions contributing to the specificity of intracellular vesicular trafficking. *Science.* 263:1146–1149.
12. Calakos, N., and R.H. Scheller. 1996. Synaptic vesicle biogenesis, docking, and fusion: a molecular description. *Physiol. Rev.* 76:1–29.
13. Cardone, M.H., B.L. Smith, W. Song, D. Mochley-Rosen, and K.E. Mostov. 1994. Phorbol myristate acetate-mediated stimulation of transcytosis and apical recycling in MDCK cells. *J. Cell Biol.* 124:717–727.
14. Casanova, J.E., P.P. Breitfeld, S.A. Ross, and K.E. Mostov. 1990. Phosphorylation of the polymeric immunoglobulin receptor required for its efficient transcytosis. *Science.* 248:742–745.
15. Casanova, J.E., G. Apodaca, and K.E. Mostov. 1991. An autonomous signal for basolateral sorting in the cytoplasmic domain of the polymeric immunoglobulin receptor. *Cell.* 66:65–75.
16. D'Esposito, M., A. Ciccodicola, F. Gianfrancesco, T. Esposito, L. Flagiello, R. Mazzarella, D. Schlessinger, and M. D'Urso. 1996. A synaptobrevin-like gene in the Xq28 pseudoautosomal region undergoes X inactivation. *Nat. Genet.* 13:227–229.
17. Dascher, C., and W.E. Balch. 1996. Mammalian Sly1 regulates syntaxin 5 function in endoplasmic reticulum to Golgi transport. *J. Biol. Chem.* 271: 15866–15869.
18. Dascher, C., J. Matteson, and W.E. Balch. 1994. Syntaxin 5 regulates endoplasmic reticulum to Golgi transport. *J. Biol. Chem.* 269:29363–29366.
19. Fiedler, K., F. Lafont, R.G. Parton, and K. Simons. 1995. Annexin XIIIb: A novel epithelial specific annexin is implicated in vesicular traffic to the apical plasma membrane. *J. Cell Biol.* 128:1043–1053.
20. Griffiths, G., and K. Simons. 1986. The trans Golgi network: sorting at the exit site of the Golgi complex. *Science.* 234:438–443.
21. Hanson, P.I., J.E. Heuser, and R. Jahn. 1997. Neurotransmitter release—four years of SNARE complexes. *Curr. Opin. Neurobiol.* 7:310–315.
22. Holthuis, J.C.M., B.J. Nichols, S. Dhruvakumar, and H.R.B. Pelham. 1998. Two syntaxin homologues in the TGN/endosomal system of yeast. *EMBO (Eur. Mol. Biol. Organ.) J.* 17:113–126.
23. Ikonen, E., M. Tagaya, O. Ullrich, C. Montecucco, and K. Simons. 1995. Different requirements for NSF, SNAP, and rab proteins in apical and basolateral transport in MDCK cells. *Cell.* 81:571–580.
24. Latterich, M., K.U. Fröhlich, and R. Schekman. 1995. Membrane fusion and the cell cycle: Cdc48p participates in the fusion of ER membranes. *Cell.* 82:885–893.
25. Leung, S.M., D. Chen, B. Das Gupta, S.W. Whiteheart, and G. Apodaca. 1998. SNAP-23 requirement for transferrin recycling in streptolysin-O permeabilized Madin-Darby canine kidney cells. *J. Biol. Chem.* In press.
26. Low, S.H., S.J. Chapin, T. Weimbs, L.G. Kömüves, M.K. Bennett, and K.E. Mostov. 1996. Differential localization of syntaxin isoforms in polarized MDCK cells. *Mol. Biol. Cell.* 7:2007–2018.
27. Low, S.H., P.A. Roche, H.A. Anderson, S.C.D. van Ijzendoorn, M. Zhang, K.E. Mostov, and T. Weimbs. 1998. Targeting of SNAP-23 and SNAP-25 in Polarized Epithelial Cells. *J. Biol. Chem.* 273:3422–3430.
28. Matlin, K.S., and K. Simons. 1983. Reduced temperature prevents transfer of a membrane glycoprotein to the cell surface but does not prevent terminal glycosylation. *Cell.* 34:233–243.
29. Mostov, K.E., and D.L. Deitcher. 1986. Polymeric immunoglobulin receptor expressed in MDCK cells transcytoses IgA. *Cell.* 46:613–621.

30. Mostov, K.E., A. de Bruyn Kops, and D.L. Deitcher. 1986. Deletion of the cytoplasmic domain of the polymeric immunoglobulin receptor prevents basolateral localization and endocytosis. *Cell*. 47:359–364.
31. Mostov, K.E., Y. Altschuler, S.J. Chapin, C. Enrich, S.H. Low, F. Luton, J. Richman-Eisenstat, K.L. Singer, K. Tang, and T. Weimbs. 1995. Regulation of protein traffic in polarized epithelial cells: the polymeric immunoglobulin receptor model. *Cold Spring Harbor Symp. Quant. Biol.* 60: 775–781.
32. Nagamatsu, S., T. Fujiwara, Y. Nakamichi, T. Watanabe, H. Katahira, H. Sawa, and K. Akagawa. 1996. Expression and functional role of syntaxin 1/HPC-1 in pancreatic beta cells. Syntaxin 1A, but not 1B, plays a negative role in regulatory insulin release pathway. *J. Biol. Chem*. 271:1160–1165.
33. Nakata, T., S. Terada, and N. Hirokawa. 1998. Visualization of the dynamics of synaptic vesicle and plasma membrane proteins in living axons. *J. Cell Biol.* 140:659–674.
34. Patel, S.K., F.E. Indig, N. Olivieri, N.D. Levine, and M. Latterich. 1998. Organelle membrane fusion: a novel function for the syntaxin homolog Ufe1p in ER membrane fusion. *Cell*. 92:611–620.
35. Pevsner, J., S.C. Hsu, J.E. Braun, N. Calakos, A.E. Ting, M.K. Bennett, and R.H. Scheller. 1994. Specificity and regulation of a synaptic vesicle docking complex. *Neuron*. 13:353–361.
36. Pimplikar, S.W., E. Ikonen, and K. Simons. 1994. Basolateral protein transport in streptolysin O-permeabilized MDCK cells. *J. Cell Biol*. 125:1025–1035.
37. Rabouille, C., T.P. Levine, J.M. Peters, and G. Warren. 1995. An NSF-like ATPase, p97, and NSF mediate cisternal regrowth from mitotic Golgi fragments. *Cell*. 82:905–914.
38. Rabouille, C., H. Kondo, R. Newman, N. Hui, P. Freemont, and G. Warren. 1998. Syntaxin 5 is a common component of the NSF- and p97-mediated reassembly pathways of Golgi cisternae from mitotic Golgi fragments in vitro. *Cell*. 92:603–610.
39. Ravichandran, V., A. Chawla, and P.A. Roche. 1996. Identification of a novel syntaxin- and synaptobrevin/VAMP-binding protein, SNAP-23, expressed in non-neuronal tissues. *J. Biol. Chem.* 271:13300–13303.
40. Rothman, J.E., and G. Warren. 1994. Implications of the SNARE hypothesis for intracellular membrane topology and dynamics. *Curr. Biol*. 4:220–233.
41. Rothman, J.E., and F.T. Wieland. 1996. Protein sorting by transport vesicles. *Science*. 272:227–234.
42. Simons, K., and E. Ikonen. 1997. Functional rafts in cell membranes. *Nature*. 387:569–572.
43. Südhof, T.C. 1995. The synaptic vesicle cycle: a cascade of protein-protein interactions. *Nature*. 375:645–653.
44. Thiery, G., J. Bernier, and M. Bergeron. 1995. A simple technique for staining of cell membranes with imidazole and osmium tetroxide. *J. Histochem. Cytochem*. 43:1079–1084.
45. Timmers, K.I., A.E. Clark, M. Omatsu-Kanbe, S.W. Whiteheart, M.K. Bennett, G.D. Holman, and S.W. Cushman. 1996. Identification of SNAP receptors in rat adipose cell membrane fractions and in SNARE complexes co-immunoprecipitated with epitope-tagged N-ethylmaleimide-sensitive fusion protein. *Biochem. J*. 320:429–436.
46. Wandinger-Ness, A., M.K. Bennett, C. Antony, and K. Simons. 1990. Distinct transport vesicles mediate the delivery of plasma membrane proteins to the apical and basolateral domains of MDCK cells. *J. Cell Biol*. 111:987–1000.
47. Weibel, E.R. 1979. Stereological methods. *In* Practical Methods for Biological Morphometry. Vol. 1. Academic Press, London. 1–415.
48. Weimbs, T., S.H. Low, S.J. Chapin, and K.E. Mostov. 1997. Apical targeting in polarized epithelial cells: there's more afloat than rafts. *Trends Cell Biol*. 7:393–399.
49. Weimbs, T., S.H. Low, S.J. Chapin, K.E. Mostov, P. Bucher, and K. Hofmann. 1997. A conserved domain is present in different families of vesicular fusion proteins: a new superfamily. *Proc. Natl. Acad. Sci. USA*. 94: 3046–3051.
50. Whiteheart, S.W., I.C. Griff, M. Brunner, D.O. Clay, T. Mayer, S.A. Buhrow, and J.E. Rothman. 1993. SNAP family of NSF attachment proteins includes a brain-specific isoform. *Nature*. 362:353–355.
51. Whiteheart, S.W., K. Rossnagel, S.A. Buhrow, M. Brunner, R. Jaenicke, and J.E. Rothman. 1994. N-ethylmaleimide-sensitive fusion protein: A trimeric ATPase whose hydrolysis of ATP is required for membrane fusion. *J. Cell Biol.* 126:945–954.
52. Wilson, K.L. 1995. NSF-independent fusion mechanisms. *Cell*. 81:475–477.
53. Wu, M.N., J.T. Littleton, M.A. Bhat, A. Prokop, and H.J. Bellen. 1998. ROP, the Drosophila Sec1 homolog, interacts with syntaxin and regulates neurotransmitter release in a dosage-dependent manner. *EMBO (Eur. Mol. Biol. Organ.) J.* 17:127–139
54. Yamasaki, S., Y. Hu, T. Binz, A. Kalkuhl, H. Kurazono, T. Tamura, R. Jahn, E. Kandel, and H. Niemann. 1994. Synaptobrevin/vesicle-associated membrane protein (VAMP) of Aplysia californica: structure and proteolysis by tetanus toxin and botulinal neurotoxins type D and F. *Proc. Natl. Acad. Sci. USA*. 91:4688–4692.